Global Change Biology (2003) **9,** 1278–1293

The annual cycles of CO_2 and H_2O exchange over a northern mixed forest as observed from a very tall tower

KENNETH J. DAVIS*, PETER S. BAKWIN†, CHUIXIANG YI*, BRADFORD W. BERGER‡, CONGLONG ZHAO§, RONALD M. TECLAW¶ and J. G. ISEBRANDS¶

Department of Meteorology, The Pennsylvania State University, 503 Walker Building, University Park, PA 16802-5013, USA, †Climate Monitoring and Diagnostics Laboratory, National Oceanic and Atmospheric Administration, 325 Broadway, Boulder, CO 80305, USA, ‡Copper Mountain Community College, 6162 Rotary Way, Joshua Tree, CA 92252, USA, §Cooperative Institute for Research in Environmental Science, University of Colorado, ¶USDA Forest Service, Forest Sciences Laboratory, 5985 Hwy K, Rhinelander, WI 54501 USA

Abstract

We present the annual patterns of net ecosystem-atmosphere exchange (NEE) of CO_2 and H2O observed from a 447 m tall tower sited within a mixed forest in northern Wisconsin, USA. The methodology for determining NEE from eddy-covariance flux measurements at 30, 122 and 396 m above the ground, and from CO_2 mixing ratio measurements at 11, 30, 76, 122, 244 and 396 m is described. The annual cycle of CO_2 mixing ratio in the atmospheric boundary layer (ABL) is also discussed, and the influences of local NEE and large-scale advection are estimated. During 1997 gross ecosystem productivity ($947-18$ g C m^{-2} yr^{-1}), approximately balanced total ecosystem respiration (963 ± 19 g C m^{-2} yr^{-1}), and NEE of CO_2 was close to zero (16 ± 19 g C m^{-2} yr^{-1} emitted into the atmosphere). The error bars represent the standard error of the cumulative daily NEE values. Systematic errors are also assessed. The identified systematic uncertainties in NEE of CO_2 are less than 60 g C m^{-2} yr^{-1}. The seasonal pattern of NEE of CO_2 was highly correlated with leaf-out and leaf-fall, and soil thaw and freeze, and was similar to purely deciduous forest sites. The mean daily NEE of CO_2 during the growing season (June through August) was -1.3 g C m^{-2} day^{-1}, smaller than has been reported for other deciduous forest sites. NEE of water vapor largely followed the seasonal pattern of NEE of CO_2, with a lag in the spring when water vapor fluxes increased before CO_2 uptake. In general, the Bowen ratios were high during the dormant seasons and low during the growing season. Evapotranspiration normalized by potential evapotranspiration showed the opposite pattern. The seasonal course of the CO_2 mixing ratio in the ABL at the tower led the seasonal pattern of NEE of CO_2 in time: in spring, CO_2 mixing ratios began to decrease prior to the onset of daily net uptake of CO_2 by the forest, and in fall mixing ratios began to increase before the forest became a net source for CO_2 to the atmosphere. Transport as well as local NEE of CO_2 are shown to be important components of the ABL CO_2 budget at all times of the year.

Keywords: annual cycle, atmospheric boundary layer budget, carbon dioxide, eddy covariance, evapotranspiration, northern mixed forest

Received 15 February 2002 and accepted 30 April 2003

Introduction

The Earth's atmospheric burden of carbon dioxide (CO_2) has been increasing at a rate of 1–2 ppm yr^{-1} over the past half-century (Conway *et al*., 1994). This increase is due to human activities, primarily the burning of fossil fuels and secondarily land use changes (Houghton, 1999). Anthropogenic emissions of CO_2 are offset in part by net uptake of CO_2 by the oceans and terrestrial biosphere. Several independent lines of evidence indicate that there is a large sink of CO_2 to terrestrial systems at north temperate latitudes. The supporting data include constraints on the atmospheric mass balance of CO_2 from atmospheric measurements and calculated ocean uptake (Tans *et al*., 1990), measurements of $\delta^{13}C$ of atmospheric CO_2 (Ciais

Correspondence: Kenneth J. Davis, e-mail: davis@essc.psu.edu

et al., 1995), and measurements of atmospheric O_2/N_2 ratio (Keeling *et al.*, 1996; Battle *et al.*, 2000), among others. However, we do not know the driving mechanisms for nor the location of this large sink. The isotope ratio ($^{13}C/^{12}C$) (Ciais *et al.*, 1995; Francey *et al.*, 1995; Bousquet *et al.*, 2000) and O_2/N_2 data (Keeling *et al.*, 1996; Battle *et al.*, 2000) also provide evidence that a significant portion of the interannual variability in the global CO_2 budget is due to variability in terrestrial biospheric sources and sinks. Recent work (Caspersen *et al.*, 2000; Pacala *et al.*, 2001) suggests that recovery of northern mid-latitude forests from logging is responsible for a majority of the terrestrial uptake in North America.

The gross exchange of CO_2 between the biosphere and the atmosphere, that is the annual cycle of growth and decay of vegetation, is very large, similar in magnitude to the ocean-atmosphere gross exchange (Schlesinger, 1997). The terrestrial sink amounts to an imbalance between the gross fluxes of only about 2–3%.

Long-term eddy-covariance flux measurements can provide direct observations of the net ecosystem-atmosphere exchange (NEE) of CO_2 (Lenschow, 1995; Goulden *et al.*, 1996a; Baldocchi *et al.*, 1988). The first annual integral of NEE of CO_2 was published by Wofsy *et al.* (1993). Since that pioneering work, observations have been conducted at a growing number of sites, many of which include at least one full annual cycle of NEE of CO_2 (see the review by Baldocchi *et al.* (2001)). Many of the studies show substantial uptake of CO_2 by the local ecosystems, which could, if representative of large portions of the Earth's ecosystems, balance the atmospheric CO_2 budget. The area represented by such measurements (order 1 km^2 from a typical surface layer tower), while large in ecological terms since it integrates across a complex mix of vegetation and soils, is quite small compared to continental scales.

Multiple-year studies of NEE of CO_2 (Goulden *et al.*, 1996b; Lindroth *et al.*, 1998; Lee *et al.*, 1999; Black *et al.*, 2000; Wilson & Baldocchi, 2001) and syntheses of results from sites spread across a continental scale (Valentini *et al.*, 2000) have also begun to appear. The interannual variability in NEE of CO_2 observed at many sites, if representative of large coherent patterns, would be large enough to explain observed interannual variability in the atmospheric CO_2 budget. Continental-scale interannual variability has yet to be examined using eddy-covariance data. This can be performed when the causes of interannual variability are coherent across large spatial scales, as is the case with climate-driven variability.

Further, eddy-covariance flux measurements are providing a rapidly growing database with which one can examine the environmental factors that govern NEE of CO_2 in various ecosystems. Such understanding enables the development of prognostic models of NEE of CO_2 at particular sites, and the ability to develop spatially comprehensive prognostic models driven by remote sensing imagery and ecological databases. Thus eddy-covariance measurements provide a basis for examining regional to continental scale NEE of CO_2 and H_2O (Running *et al.*, 1999; Mackay *et al.*, 2002; Baker *et al.*, this issue; Denning *et al.*, this issue).

This paper presents the annual cycle of NEE of CO_2 during 1997 for a mixed northern forest as observed from a 447 m tall television transmitter tower located in the Chequamegon National Forest of northern Wisconsin, USA. We present a methodology for deriving our best estimate of NEE from flux measurements at multiple levels on the tower and discuss the random and systematic uncertainty in NEE of CO_2. We then describe the relationship between NEE of CO_2 at this site and environmental factors, in particular photosynthetically active radiation (PAR), temperature, and seasonal factors including leaf cover (phenology) and soil thaw. This study is unique in that the area represented by these NEE observations, also known as the flux footprint, is unusually large, as much as 100 times larger than that of a typical surface-layer flux tower. The vegetation cover is heterogeneous, including mature upland deciduous and coniferous forests, deciduous and coniferous wetlands, and recently logged uplands dominated by young aspen. This study is also unique in its use of the multiple-level flux measurements to examine systematic errors in our estimates of NEE of CO_2, and in the joint evaluation of the seasonal cycles of both NEE of CO_2 and the atmospheric boundary layer (ABL) CO_2 mixing ratio.

Materials and methods

Research site and instrumentation

The WLEF television (TV) tower is located in the Park Falls Ranger District of the Chequamegon National Forest about 15 km east of Park Falls, Wisconsin, USA, at 45.9459°N latitude, 90.2723°W longitude. It is located in a region of low relief: typical hilltop to valley elevation change is about 20 m with undulations in terrain that occur over spatial scales of a few hundred meters. The elevation changes create a heterogeneous landscape of saturated (wetland) and unsaturated (upland) soils. The landscape is managed. Logging activities include thinning and clear-cuts, and are concentrated in the upland regions. The fraction of forest within the tower footprint that is cut in any one year is small, but a significant fraction of the landscape has experienced some cutting or thinning within the

past few decades. The whole region was heavily logged around the beginning of the 20th century, similar to many forests in the north central United States.

Species of trees found in the upland regions include aspen, balsam fir, sugar maple, red maple, basswood, red pine, paper birch, yellow birch, and white spruce. Recent clear-cuts are dominated by dense aspen, while older stands tend to be dominated by sugar maple or red pine. Wetlands comprise about 40% of the surrounding landscape and include alder, cedar, tamarack, and black spruce stands. Mackay *et al.* (2002) document the regional forest cover in more detail. Maximum canopy height in the region is about 25 m. Wetlands tend to have substantially lower canopies as do young aspen stands. Soils are sandy loam and are mostly glacial outwash deposits. The site is at the northern edge of the Mississippi River Basin.

The WLEF TV tower is instrumented for eddy-covariance fluxes at 30, 122, and 396 m. Fluxes of water vapor, virtual temperature, CO_2, and momentum are measured using sonic anemometers and closed-path infrared gas analyzers (IRGAs). In 1997 there were Applied Technologies, Inc. (Longmont, Colorado, USA), 3-D K-type sonic anemometers at 30 and 396 m and a Campbell Scientific, Inc. (Logan, Utah, USA), CSAT3 sonic at 122 m. CO_2 and H_2O mixing ratios were measured by LI-COR (Lincoln, Nebraska, USA), 6262 IRGAs located in a trailer at the base of the tower. The flux measurement methodology is described in detail by Berger *et al.* (2001). High-precision, high-accuracy CO_2 mixing ratio measurements were made at 11, 30, 76, 122, 244, and 396 m using a LI-COR 6251 IRGA located in the trailer (Zhao *et al.*, 1997; Bakwin *et al.*, 1998). These measurements were used to both calibrate the fast-response IRGAs used for eddy-covariance flux measurements, and to calculate the rate of change of storage in the column of CO_2.

Method of computing NEE of CO_2

In this paper, we follow the typical assumption that the NEE of CO_2 can be described as the sum of the turbulent flux plus the rate of change of storage. That is, we take the equation for NEE where all horizontal components are assumed to be aligned along the (u, x) direction,

$$\mathrm{NEE} = \int_0^{z_r} \left(\frac{\partial \bar{c}}{\partial t} + \frac{\partial \overline{u'c'}}{\partial_{xg}} + \bar{u}\frac{\partial \bar{c}}{\partial x} + \bar{w}\frac{\partial \bar{c}}{\partial z} \right) \mathrm{d}z + \overline{w'c'}_{z_r}, \quad (1)$$

and simplify by assuming that the horizontal transport and vertical advection terms are negligible for long-term averages yielding,

$$\mathrm{NEE}_0 = \int_0^{z_r} \frac{\partial \bar{c}}{\partial t}\,\mathrm{d}z + \overline{w'c'}_{z_r} = F_{C_{st}} + F_{C_{tb}}, \quad (2)$$

where the subscript 0 emphasizes that this is an approximation that depends on the transport being one-dimensional (Yi *et al.*, 2000). The CO_2 mixing ratio is denoted by c, z is the altitude above ground, and w is the vertical velocity. Variables are broken down into time-averaged mean (denoted by an overbar) and fluctuating components (primed). The turbulent flux measured via eddy covariance is $\overline{w'c'}_{z_r}$ where z_r is the height of the flux measurement. We use an averaging time of 1 h for our calculations (Berger *et al.*, 2001). The assumptions made to reach Eqn (2) do not hold true for all individual hours. We assume that only when averaged over many synoptic cycles the horizontal transport and vertical advection terms are unimportant.

Since turbulent fluxes are measured at three different altitudes on the WLEF tower it is possible to derive three estimates of NEE_0 when all instruments are operational. Intercomparison among levels provides a means of examining the uncertainty in tall tower observations of forest–atmosphere CO_2 exchange. If the surface flux is homogeneous within the footprint of all three flux measurements and advection of CO_2 is negligible (i.e. $\mathrm{NEE} = \mathrm{NEE}_0$), then NEE_0 will be identical for all three possible z_r. To the degree that NEE_0 is not identical at all levels, we test the robustness of our results with respect to these sources of uncertainty.

In practice, the multiple levels are also used interchangeably to compute NEE_0 when data are missing at any one preferred level, thus comparisons of data from different times must be viewed with caution if data from different levels are used. Finally, we hypothesize that a regular switching among levels as a function of atmospheric stability provides the best estimate of regional forest-atmosphere NEE of CO_2. We examine the long-term average of NEE_0 at the three observation levels in order to identify any systematic biases prior to presenting our best estimate of NEE.

Optimal algorithm for computing NEE of CO_2

Three factors define the optimal algorithm for deriving NEE from the three flux measurements. First, there is a clearing around the tower with a radius of roughly 200 m. Under stable atmospheric conditions, footprint studies indicate that it is unlikely that this clearing will strongly influence the flux measurements at any level (Horst & Weil, 1992; Weil & Horst, 1992). Under strongly convective conditions it is likely that the 30 m level could be significantly influenced by the clearing, while measurements at the 122 and 396 m levels will be little affected by the clearing.

A second practical concern is the depth of turbulent mixing. It is well established that when turbulent mixing is weak and the contribution of $F_{C_{st}}$ to NEE_0 is large there is often a systematic underestimate of NEE,

possibly due to drainage flows that remove CO_2 via horizontal and vertical advection (Lee, 1998; Finnigan, 1999; Massman & Lee, 2002). Therefore we want to maximize our use of eddy-covariance flux data, and minimize our reliance on measurements of $F_{C_{st}}$. Typically the 396 m level is turbulent only during daytime convective conditions. At night the flow is often laminar and the 396 m level is completely decoupled from the Earth's surface. The 30 m level is almost always turbulent, except under extremely calm, stable conditions. The 122 m level is often turbulent at night, but is near the top of the night-time boundary layer (Yi *et al*., 2001). Figure 1 illustrates this pattern by showing vertical velocities at each level for a typical day overlaid on a radar reflectivity plot illustrating the depth of turbulent mixing. Also shown is the diurnal pattern of CO_2 mixing ratios observed on the same day.

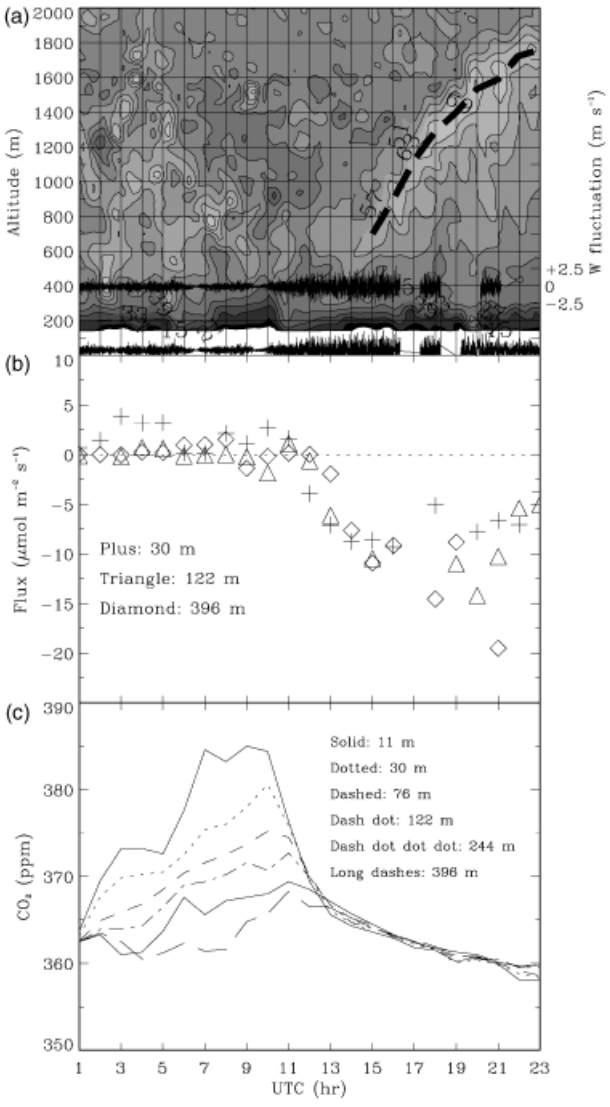

Finally, stability has a strong influence on the footprint of a turbulent flux measurement. Strongly convective conditions lead to relatively small footprint regions since vertical velocities become comparable to horizontal velocities (Weil & Horst, 1992). Typical fetches of flux footprints under strong convection are roughly 10 times the altitude of the turbulent flux measurement. Stable conditions lead to much larger flux footprints since vertical mixing becomes weak (Horst & Weil, 1992). Upwind fetches of flux footprints are order of 100 times greater than the altitude of a flux measurement in neutral to stable conditions. Thus, any one eddy-covariance flux measurement, fixed at a single altitude, suffers over the course of a typical day from an order of magnitude change in flux footprint. The multiple flux measurements at the WLEF tower, differing in altitude by more than a factor of 10, can be selected as a function of stability such that the flux footprint for NEE_0 is more steady than is possible with a single measurement altitude.

The optimal algorithm for computing NEE of CO_2 consists, therefore, of using the 30 m measurements of $F_{C_{tb}} + F_{C_{st}}$ when conditions are stable and some combination of the 122 and 396 m measurements when conditions are unstable. This maintains a large footprint while also maximizing the fraction of the flux measured by eddy covariance and avoiding the influence of the

Fig. 1 Data from the WLEF observational array covering one daily cycle, 22 May 1998. Conditions were clear and calm. Local standard time is UTC – 6 h. (a) Radar reflectivity from a 915 MHz radar operated by the National Center for Atmospheric Research near the WLEF tower (Yi *et al*., 2001). The dotted line shows the convective boundary layer top, identified by the region of high reflectivity. Overlaid on the reflectivity plot are the vertical winds measured by the sonic anemometers at 30 and 396 m, plotted at the appropriate altitude relative to the radar reflectivity data. The transition from stable night-time to convective daytime conditions is evident, as is the very large change in mixing depth that occurs. Note that radar reflectivity data are not available below about 200 m. (b) Hourly turbulent flux of CO_2, F_{tb}, measured on the WLEF tower for the same day. Note upwards flux, driven by respiration at night, only evident at the lower levels, and downwards flux, driven by net photosynthesis during the day and evident at all levels. (c) CO_2 concentrations from all 6 levels. Note the highly stratified layers and large accumulation of CO_2 at night, contrasted by the well-mixed conditions and relatively small depletion of CO_2 during the day. This asymmetry in mixing ratio is driven by the covariance between mixing depth and fluxes shown in (a) and (b) During the day the deep mixing makes it difficult to deplete boundary layer CO_2 mixing ratios while shallow mixing at night leads to large accumulation. It is also evident that the morning turbulence transition (11–13 UTC or 5–7 LST) leads to a large and rapid time rate of change of CO_2 concentration.

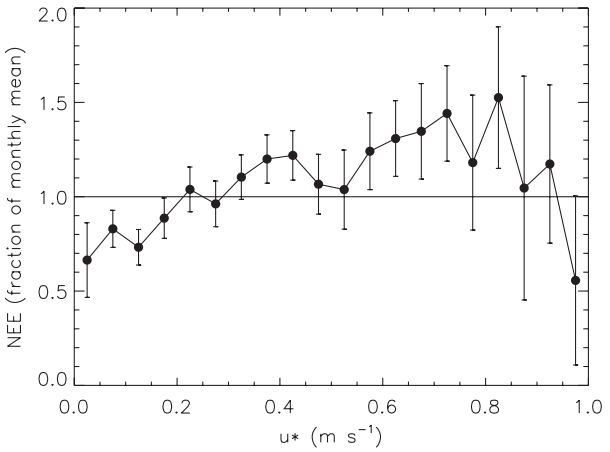

Fig. 2 Normalized night-time NEE_0 of CO_2 for 1997 from WLEF plotted vs. u_*. Data are normalized by the monthly mean nighttime NEE_0. The bars indicate standard error for a population of hourly measurements. Data are from 30 m, the primary level used for night-time flux measurements.

clearing around the tower. We must consider, however, non-ideal behavior such as horizontal advection in making the best possible NEE estimate.

Advection during the morning transition

Yi *et al.* (2000) used the measurements at multiple levels on the WLEF tower to assess the influence of advection on measurements of NEE_0. They found that, as a monthly mean, advection is usually negligible except during the morning transition from stable to turbulent conditions. Yi *et al.* (2000) showed that during July 1997, NEE_0 from 30 m measurements is about 25% less negative than from 122 or 396 m. This difference is greatest after calm nights when a great deal of CO_2 accumulates close to the ground and is vented at the onset of turbulence. Most of the uptake at this time does not come from the rate of change of storage ($F_{C_{st}}$). The 122 m and 396 m NEE_0 data suggest a peak value of net uptake early in the morning that is difficult to reconcile with the environmental parameters that dominate the diurnal course of NEE of CO_2 (PAR, soil temperature). This result is similar to the observations of Anthoni *et al.* (1999) (their Fig. 2) at a forested site in much more complex terrain. The morning uptake at their site was much too large to explain via environmental variables and they chose to discard these data.

We reach a similar conclusion. While it is possible that the upper level measurements simply represent a larger footprint than the 30 m data, it is more plausible, in our opinion, that the venting of CO_2 during the morning transition occurs in a way that is not completely captured by the turbulent flux measurements. This would cause an error in NEE at all levels, but the error would be minimized at 30 m since the storage flux contribution to NEE_0 is proportional to height above ground. Under this assumption, Yi *et al.* (2000) estimated that morning advection at 30 m would yield a 10% overestimate of diurnally integrated net uptake in July of 1997. This hypothesis is consistent with our finding that soil temperature and PAR do not explain the large morning uptake, and is strengthened by the similar findings of Anthoni *et al.* (1999). The counterargument (these data are valid and the upper level data are showing, for instance, a response to afternoon vapor pressure deficit) would require that morning NEE of CO_2 is enhanced after calm nights, which seems unlikely. The impact of our exclusion of these data is quantified in Table 1.

Low friction velocity conditions

Stable conditions, typical of night-time, are often troublesome for NEE measurements based on Eqn (2). Drainage flows may draw cool surface air downslope at

Table 1 NEE of CO_2 for June through August of 1997 from various levels as observed from the WLEF tower representing integrals of portions of Fig. 3

	Fraction of preferred NEE_0			Preferred NEE_0
Time of day	NEE_0 at 30 m	NEE_0 at 122 m	NEE_0 at 396 m	(g C m^{-2} day^{-1})
Whole day	0.89	1.18	1.08	−2.25
Whole day with 6–9 LST replaced by 30 m fluxes		0.98	0.96	
AM transition (5–10 LST)	0.98	1.29	1.16	−1.87
Daytime (11–14 LST)	0.90	0.94	1.06	−2.01
PM transition (15–18 LST)	1.004	1.01	1.16	−0.58
Night (19–4 LST)	1.00	1.01	1.15	2.21

Data include only hours where data from all three flux levels are available, and low u_* data have not been screened out. As a result, the daily NEE presented here differs from the mean rate of summer uptake shown in Fig. 11 and noted in the abstract.

these times and turbulent transport is intermittent. It has become common practice to examine NEE_0 as a function of the friction velocity, u_*, and search for a threshold value below which the NEE_0 measurements are thought to be in error (Goulden *et al.*, 1996a; Aubinet *et al.*, 2000; Pawu *et al.*, 2000; Schmid *et al.*, 2000; Falge *et al.*, 2001). The hypothesis is that night-time respiration should not depend on u_*, so the commonly observed fall-off of NEE_0 at low u_* is evidence of systematic bias. A threshold value for u_* of about $0.2\,m\,s^{-1}$ is typical.

We examine night-time NEE_0 at 30 m vs. friction velocity at WLEF to determine a threshold u_* at which the NEE_0 should be discarded. Figure 2 shows a gradual decrease of NEE_0 as a function of u_* which could be interpreted as starting at $u_* = 0.7\,m\,s^{-1}$, a much larger value than is typical for a site with very low relief such as WLEF. For the nearby Willow Creek site, located on a gentle slope, Cook *et al.* (in prepration) show a more distinct drop-off when u_* is below $0.15\,m\,s^{-1}$. Given the very flat, but heterogeneous landscape, at WLEF it is possible that the windy conditions lead to increased transport of CO_2 to the site at night, while calm conditions are correlated with some drainage. Preliminary measurements on a calm morning with a backpack-borne LI-COR IRGA showed pooling of CO_2 at 1 m level in the wetlands around WLEF. The net effect, however, is modest, and it is most pronounced for $u_* < 0.2\,m\,s^{-1}$ (Fig. 2). We will examine our results with and without a minimum threshold u_* value of $0.2\,m\,s^{-1}$. The u_* threshold is only applied at night; daytime convection should generate enough mixing to prevent substantial drainage flow even for small u_* values.

Algorithm for computing NEE of CO_2

If data from all flux levels are present we switch among levels according to stability, and use the sensible heat flux (H) as our indicator of stability. For H less than $100\,W\,m^{-2}$ we use 30 m data. Thus we take advantage of the maximum amount of nonzero night-time $F_{C_{tb}}$ data and minimize bias due to the hypothesized advection during the morning transition when H is between 10 and $100\,W\,m^{-2}$. This somewhat arbitrary $100\,W\,m^{-2}$ threshold includes nearly all the morning hours when the contribution of $F_{C_{tb}}$ from 122 and 396 m is anomalously large. When H is greater than $100\,W\,m^{-2}$ (vigorous mixing and relatively small flux footprints), we use an average of the fluxes obtained from the 122 and 396 m levels. If data are missing from either one of these two levels, we use data from the remaining upper level. If both upper levels are missing under unstable conditions, we use 30 m data. If data from 30 m are missing under stable conditions, we use 122 m data and, if that is missing as well, we use 396 m data. Only when data from all three levels are absent do we fill in with an empirical fit based on environmental conditions.

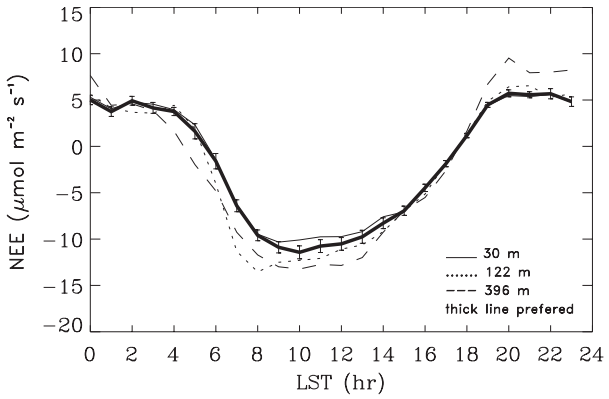

Fig. 3 NEE_0 of CO_2 is plotted vs. time of day for each flux level at WLEF, showing the comparison among the three flux levels. The plot shows a mean diurnal pattern of all hours from June through August of 1997, where data are available from each level. Night-time low u_* data have not been screened out. Also shown is the result of the algorithm for extracting our preferred estimate of NEE_0 (see text). Note that fluxes reported for hour j represent the average flux for the time interval from hour j to hour $j+1$. This convention is used throughout the paper.

The results of this algorithm for the growing season of 1997 are shown in Fig. 3. It is evident that 30 m data are used for the majority of the night when stable or only weakly unstable conditions dominate, while daytime fluxes are taken more often from the 122 and 396 m levels. This plot also allows us to examine the uncertainty in NEE of CO_2 revealed by our multiple flux measurements.

The data in Fig. 3 are summarized for four times of the day in Table 1. These data show that the choice of any one level is within 20% of the preferred value for the daily integral of NEE of CO_2, with NEE at 30 m showing 11% less net uptake than our preferred value of $-2.25\,g\,C\,m^{-2}\,day^{-1}$ and the 122 and 396 m levels showing 18% and 8% larger uptake, respectively. Most of the difference is explained by the anomalously large uptake during the morning transition at the upper levels, as discussed by Yi *et al.* (2000) and evident between hours 6 and 10 LST in Fig. 3. If 6-9 LST data (through the end of hour 9, 4 h total) at 122 and 396 m are replaced with 30 m data, then the differences between these levels and our preferred value drops to only 2% and 4%, respectively. The remaining differences between the preferred value and the individual levels are low uptake at 30 m during the day, high uptake at 396 m during the afternoon transition hours, and larger respiration at 396 m during night-time hours.

The 396 m differences are offsetting in the daily sum. Daytime fluxes from the 30 m level should be viewed with suspicion due to the influence of the clearing around the tower. Night-time respiration data from 396 m are similarly suspect since the measurement is almost entirely $F_{C_{st}}$. In conclusion, we find that the multiple altitude measurements of NEE of CO_2 are consistent to within 15% or better at various times of day and to within 5% for the daily integral, or ≤ 10 g C m^{-2} if integrated over 100 days of the growing season. These micrometeorological patterns should be similar at times of the year other than the growing season.

Methodology for filling missing data

Continuous eddy-covariance flux measurements incorporate fairly complex instruments operating in remote and sometimes harsh environments. The WLEF tower is particularly challenging because of the logistics of servicing instruments on the tower, and frequent harsh conditions especially at the upper measurement levels. Sonic anemometers have proven the most difficult to maintain, with Campbell Scientific CSAT-3's proving more durable than Applied Technologies Inc. instruments, but losing somewhat more data to dewy conditions. Three flux levels provide greater data coverage than would otherwise be possible, but gaps with no valid flux data still exist. In 1997, 75% of hours had turbulent flux measurements from at least one level. Individual levels (30, 122, 396 m) measured turbulent fluxes 67%, 59%, and 35% of the time, respectively. Thirteen percent of the night-time flux data are from hours where u_* is below the threshold value of 0.2 m s^{-1}. If these data are eliminated, 66% of the hours in 1997 are characterized by valid turbulent flux measurements.

Small data gaps of one to two hours are filled by linear interpolation. Gaps of 3 h up to 2 weeks are filled using empirical fits to 5 cm soil temperature (T_s) and incident photosynthetically active radiation (PAR), similar to the methods described by Falge *et al.* (2001). We assume that ecosystem respiration can be fit by T_s, and that photosynthesis can be fit by PAR. Large gaps or gaps where no environmental data (e.g. T_s or PAR) are available are filled with a median daily pattern taken from 2 weeks before and after the period of missing data. There is no significant systematic bias in PAR or T_s between periods when we have good eddy flux data and periods when we do not. No substantial bias exists when choosing among soil temperatures close to the surface or surface air temperature for the empirical fit with ecosystem respiration.

Net ecosystem exchange of CO_2 (NEE) is decomposed into the difference between gross ecosystem productivity (GEP) and total ecosystem respiration (RE),

$$\mathrm{NEE} = \mathrm{RE} - \mathrm{GEP}, \tag{3}$$

where our sign convention is such that the positive NEE is a flux of CO_2 into the atmosphere and both RE and GEP are positive. We use the relationship

$$\mathrm{RE} = a_0 \exp^{a_1(T_s - a_2)} \tag{4}$$

to fit the response of RE to temperature changes (Lloyd & Taylor, 1994; Falge *et al.*, 2001), where a_0, a_1 and a_2 are empirical parameters fit for each calendar month. Data for the fits are taken from night-time NEE_0 measure-

Table 2 Parameters derived from monthly fits of RE and GEP data (see Eqn (3)) to respiration and photosynthesis functions (Eqs (4) and (5)) and the uncertainty in the parameters (σ values)

	Respiration parameters						Photosynthesis parameters					
Month	a_0	σ_{a_0}	a_1	σ_{a_1}	a_2	σ_{a_2}	b_0	σ_{b_0}	b_1	σ_{b_1}	b_2	σ_{b_2}
1	207	1154	1.24	0.17	5.6	0.6	1.10	0.34	2.2	1.3	0.99	0.34
2	6.3	7.0	0.158	0.067	17.8	2.4	0.99	0.08	1.7	0.7	1.00	0.08
3	1.8	1.1	0.049	0.020	29.7	5.2	1.35	0.08	18.3	2.3	1.16	0.08
4	1.8	8.6	0.021	0.009	29.7	4.4	1.26	0.02	256	9	−0.28	0.02
5	4.7	1.9	0.087	0.004	20.6	2.0	4.15	0.02	328	7	0.13	0.02
6	6.8	8.0	0.101	0.001	15.6	1.6	16.46	0.01	229	1	−0.34	0.02
7	6.7	0.6	0.131	0.001	16.3	1.5	27.42	0.02	359	1	2.69	0.02
8	6.7	0.4	0.150	0.002	16.1	2.0	24.28	0.03	436	3	0.57	0.03
9	6.8	1.8	0.092	0.001	16.3	1.3	17.20	0.02	314	2	−0.42	0.03
10	4.9	1.7	0.033	0.001	21.2	1.6	7.18	0.03	294	7	−0.70	0.04
11	1.3	0.2	0.018	0.004	41.5	2.7	1.09	0.19	34.7	6.3	0.70	0.19
12	61.9	7.3	0.686	0.022	8.6	0.6	0.95	0.54	−6.1	3.1	0.79	0.54

Units for a_0, b_0, and b_2 are μmol C m^{-2} s^{-1}; a_1 is °C^{-1}; a_2 is °C; b_1 is μmol PAR m^{-2} s^{-1}.

ments, assuming that in the absence of sunlight NEE = RE. A second relationship,

$$\mathrm{GEP} = \mathrm{RE} - \mathrm{NEE} = -b_2 + \frac{b_0 \mathrm{PAR}}{(\mathrm{PAR} + b_1)}, \qquad (5)$$

fits GEP and PAR data using empirical parameters b_0, b_1 and b_2. This function reproduces a light-limited and light-saturated regime for photosynthesis (Falge *et al.*, 2001). Table 2 shows the variability of these coefficients over the entire year for the WLEF site. The fit parameters from this table and PAR and T_s data were used to fill in the one-third of NEE data that are missing or falls below our night-time u_* threshold.

Results

Climate

The climate for the region around the WLEF tower in 1997 was similar to 30-year climatic means. The mean annual temperature for 1997 at the National Climatic Data Center surface station at Park Falls (4.7 °C) was close to the mean for 1967–1996 (4.6 °C). Total precipitation measured at Park Falls in 1997 was 668 mm, about 80% of the 30-year mean of 832 mm, but given the high spatial and temporal variability of precipitation this difference may not be significant. The mean annual temperature and precipitation recorded at WLEF in 1997 were 4.9 °C and 711 mm, respectively. A plot of environmental conditions for the year is shown in Fig. 4. Several dates are particularly notable. Soils thawed at approximately day 104 (14 April), and froze on about day 315 (11 November). Dates of leaf-out and leaf-fall are evident in the plot of the fraction of intercepted PAR, determined from the ratio at noon of below-canopy to above-canopy PAR at a deciduous site near the WLEF tower. Intercepted PAR rises rapidly around day 151 (30 May) to nearly full interception and drops nearly as rapidly about day 283 (10 October), for a leaf-covered season of approximately 132 days. Leaf-out and leaf-fall follow and precede soil thaw and freeze. The mean daytime vapor pressure deficit, derived from 30 m air temperature and humidity data, peaks around the time of leaf-out, which is also the time of maximum incoming solar radiation. Daytime mean vapor pressure deficits are modest, and growing season precipitation exceeded evapotranspiration in 1997 (see below).

CO_2 exchange

Unlike the Willow Creek site (Cook *et al.*, unpublished results), no striking dependence of fluxes vs. wind direction was found at WLEF. Figure 5a shows the time

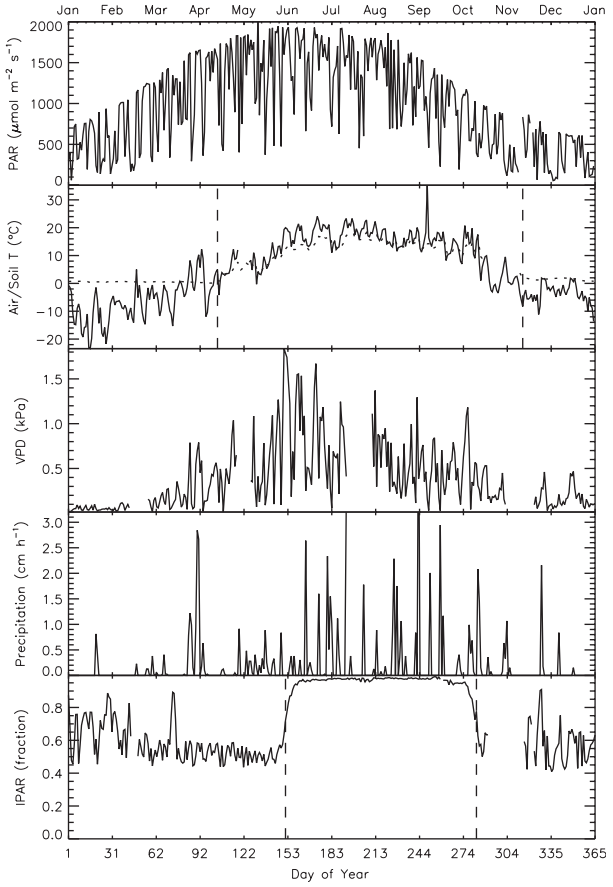

Fig. 4 Climatological conditions as observed at the WLEF tower and a nearby deciduous canopy research site (Willow Springs) during 1997. The first plot shows the daily maximum incoming photosynthetically active radiation (PAR). All other plots are daily means. 30 m air temperature (122 m when 30 m data are missing) and 5 cm soil temperatures, daytime vapor pressure deficits at 30 m, daily total precipitation (three different tipping buckets are used because of missing data at various times), and the fraction of intercepted PAR for a deciduous canopy are shown. Note that snowfall is very poorly measured by the tipping buckets, and likely represents a significant underestimate. Vertical lines on the soil temperature and intercepted PAR plots show approximate dates of soil thaw/freeze and leaf-out/senescence, respectively.

series of hourly preferred NEE for 1997. It is evident that both respiratory and photosynthetic fluxes are greatly enhanced while deciduous trees are in leaf within the WLEF footprint. Flux magnitudes are also somewhat enhanced above the winter values in the period when the soil is thawed but prior to leaf-out. Figure 5b shows the hours where data have been filled with either the soil temperature and PAR empirical fits or a monthly diurnal mean.

Figure 6 shows the monthly median NEE of CO_2 vs. time of day. Months with snow-covered and frozen

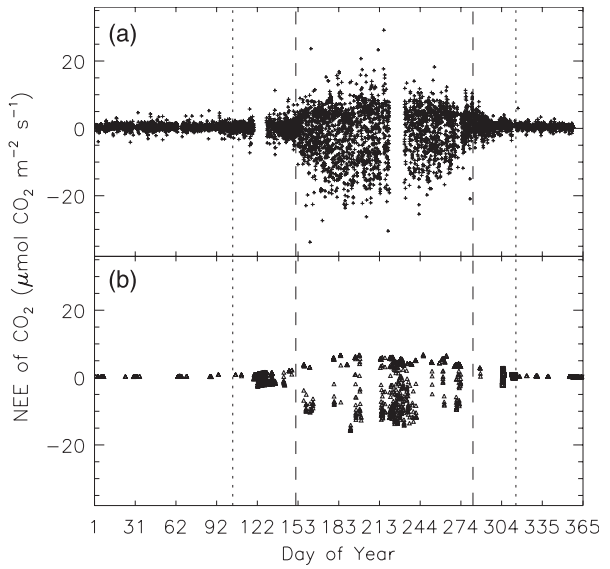

Fig. 5 Hourly net ecosystem exchange of CO_2 for 1997 as measured by the WLEF tower. Data points represent our preferred hourly fluxes selected from among the three flux levels by the algorithm described in this paper. Also noted are the approximate times of soil thaw/freeze (dotted vertical lines) and leaf-out/senescence (dashed vertical lines). Gaps are due to missing flux data. Night-time fluxes when u_* values are less than $0.2\,m\,s^{-1}$ have been screened out. The top panel shows observed hourly fluxes vs. day of the year, and the bottom panel shows the filled fluxes.

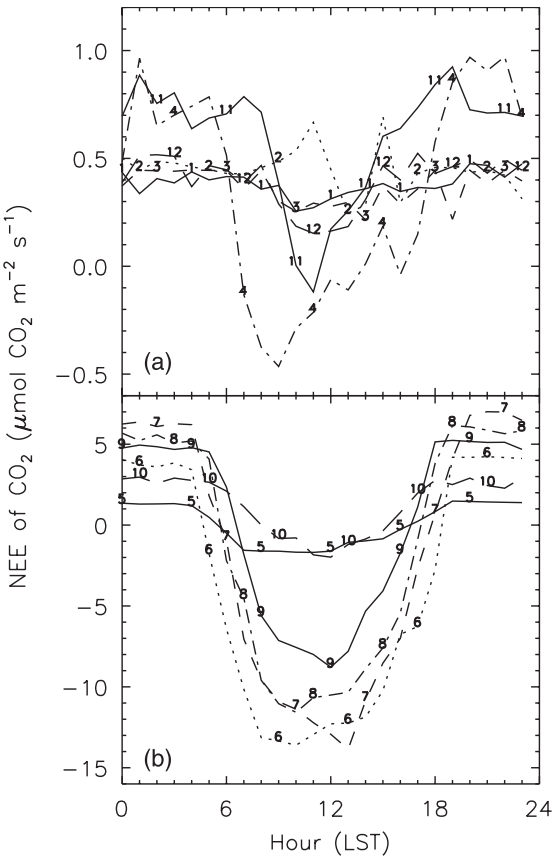

Fig. 6 Monthly median diurnal pattern of NEE_0 of CO_2 for 1997 observed at the WLEF tower. Results are the preferred NEE_0 values as described in the text, and include only direct observations, not data filled using T_s–PAR relationships or median diurnal patterns. Low u_* night-time fluxes are not included. The months are divided into two plots according to the magnitude of observed NEE_0, roughly matching (a) the dormant season and (b) the growing season. The curve for each month is labelled numerically where 1 = January, 2 = February, etc.

soils (December through March) show small respiratory fluxes of about $0.5\,\mu mol\,C\,m^{-2}\,s^{-1}$ throughout the day. Slight depressions of this rate (roughly $0.1\,\mu mol\,C\,m^{-2}\,s^{-1}$) are observed at mid-day even in winter months, perhaps due to evergreen photosynthesis on warmer, sunny winter days. April and November, which include the transitions from frozen, snow covered conditions to exposed, thawed soils and back show substantially larger respiratory and photosynthetic fluxes than the winter months, but the amplitude is still very small compared to the summer months. May and October, both months when the soils are thawed but leaves are generally not present on the deciduous trees, show modest photosynthetic activity ($NEE \simeq -1\,\mu mol\,C\,m^{-2}\,s^{-1}$), and October in particular shows increased respiratory fluxes. During the growing season, the net uptake of CO_2 peaks in June and July (maximum monthly NEE is about $-13.5\,\mu mol\,C\,m^{-2}\,s^{-1}$), while night-time respiratory fluxes peak somewhat later in July and August ($NEE \simeq 6$–$7\,\mu mol\,C\,m^{-2}\,s^{-1}$). The months with maximum photosynthetic activity, June through September, are consistent with the dates of leaf-out and leaf-fall seen in Fig. 4.

Both RE and GEP peak in July at $+6.7$ and $8.5\,g\,C\,m^{-2}\,day^{-1}$, respectively (Fig. 7). RE stays somewhat elevated in September and October while GEP falls off more rapidly, resulting in a June through August minimum in monthly mean NEE. The summer (June through August) mean daily rate of uptake varies from -1.0 to $-1.7\,g\,C\,m^{-2}\,day^{-1}$. The standard error of the summer daily uptake rate, averaged over a single month, is about $0.3\,g\,C\,m^{-2}\,d^{-1}$. This does not address potential systematic errors, but does include random variability due to weather, instrumental noise, and atmospheric turbulence. Net fluxes in September are slightly positive, and the largest positive monthly mean NEE occurs in October, at $1.4\,g\,C\,m^{-2}\,d^{-1}$. Winter net emissions are about $0.4\,g\,C\,m^{-2}\,d^{-1}$.

The summer uptake rate at WLEF is substantially smaller than the rates for other temperate deciduous forests that tend to cluster around $-4\,g\,C\,m^{-2}\,day^{-1}$

(D. Hollinger, personal communication). We hypothesize that this is due to the extensive wetlands in the footprint of the WLEF tower. This hypothesis in supported by the larger summer uptake rate found at Willow Creek, a homogeneous mature deciduous upland forest in the region (Cook *et al.*, unpublished results). Forest management in the footprint of the WLEF tower may also contribute to this difference. It is interesting to note that 2000 Willow Creek data (Cook *et al.*, unpublished results) suggest that the difference in NEE of CO_2 between WLEF and Willow Creek is mostly caused by higher RE values at WLEF. However, weather conditions were substantially different in these two years, with more fair conditions in 1997. This intercomparison will be more carefully addressed in future analyses using data from the same calendar year.

The annual sums of NEE, GEP, and RE are summarized in Table 3, which also presents the sensitivity of these results to the inclusion of low u_* night-time flux data and the use of a monthly median to replace all missing flux data rather than the T_s-PAR fits described previously. These analyses give some sense of the potential magnitude of systematic errors in these long-term integrals. The propagated random uncertainty in our annual sum of NEE of CO_2 is found to be large compared to our NEE value, but relatively small compared to NEE values found at other temperate deciduous forest sites that are often in the range of -100 to $-300\,\mathrm{g\ C\,m^{-2}\,yr^{-1}}$ (Goulden *et al.*, 1996b; Valentini *et al.*, 2000; Baldocchi *et al.*, 2001). The standard errors in GEP and RE are very small compared to the annual integrals of these values. Note that these standard errors are derived from observed variability in the integrated flux measurements, and therefore include random errors inherent to sampling turbulent quantities such as fluxes, as well as variability caused by time-varying ecosystem-atmosphere exchange. These error bounds, therefore, should not be interpreted as comprehensive uncertainty estimates.

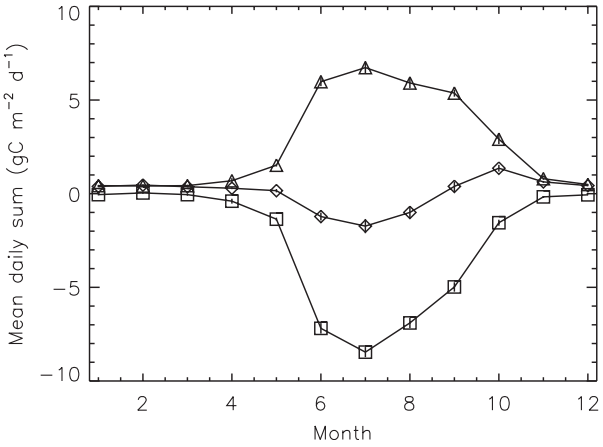

Fig. 7 Monthly mean values of the daily integrals of NEE, GEP, and RE of CO_2 for 1997 as computed using data from the WLEF tower. Error bars are the standard errors computed from the monthly ensemble of daily measurements. Low u_* data have been screened, and all hours of the year are represented meaning that some data are from monthly T_s–PAR fits. Triangles (positive values) represent RE and squares (negative values) represent -GEP. The sum is NEE of CO_2 and is shown by the diamonds.

Screening low-turbulence data ($u_* < 0.2\,\mathrm{m\,s^{-1}}$) at night makes a significant difference in the annual NEE, GEP, and RE values (Table 3). If the data are not screened to eliminate very stable periods, the estimated total respiration (RE) decreases by about 15%, GEP is reduced, and NEE is $64\,\mathrm{g\ C\,m^{-2}\,yr^{-1}}$ more negative than our best estimate. The choice of data filling method (fits to T_s and PAR vs. monthly median diurnal cycles) makes little difference. The conclusion that the WLEF region was roughly neutral with respect to the annual NEE of CO_2 for 1997 is robust for all the permutations of data analysis that we have examined.

It is worth noting that even screening of low u_* data typically does not balance the surface energy budget at tower flux sites (Massman & Lee, 2001), leaving open the possibility that CO_2 flux magnitudes are systematically underestimated at all times. For example, Twine *et al.* (1999) suggest increasing the magnitude of all CO_2 fluxes by the same amount required to balance the surface energy budget by increasing H_2O fluxes. We do not examine this suggestion here. If systematic underestimation of CO_2 flux magnitudes at all times is occurring, determining the magnitude of this error as a function of atmospheric stability will prove critical in

Table 3 Annual sums of NEE, RE, and GEP of CO_2 for 1997 as computed at the WLEF tower using various methods and Eqns (3)–(5); the σ values are standard errors computed by propagating the standard errors in the monthly means shown in Fig. 7

	($\mathrm{g\ C\,m^{-2}\,yr^{-1}}$)					
Method of computing cumulative fluxes	NEE	σ_{NEE}	GEP	σ_{GEP}	RE	σ_{RE}
Night-time low u_* screened, T_s–PAR fill	16	19	947	18	964	19
No u_* screening	−48	20	864	18	816	21
Median fill, low u_* screened	18	16	951	16	968	15

determining the absolute accuracy of our measurements of NEE of CO_2 since NEE is the difference of two large gross fluxes, GEP and RE, and GEP is highly correlated with atmospheric stability.

Evapotranspiration and energy balance

Fluxes of CO_2 and H_2O are closely linked. In this section we describe the basic aspects of the annual cycle of NEE of H_2O of this mixed forest environment including the surface energy balance, seasonal patterns in the diurnal cycle of latent heat fluxes (LE), the net daily energy fluxes at the site, and the mid-day Bowen ratios. Note that in this section only the turbulent flux measurements are used; the rate of change of storage of water vapor and temperature are not included. Also, we have not filled missing energy flux data as we did with the empirical algorithm for CO_2 fluxes.

The surface energy balance has been used as a test of the turbulent energy fluxes from eddy-covariance experiments. Computing the surface energy balance at WLEF is problematic because net radiation is measured over the clearing around the tower, and these data are certainly not representative of the mixed forest/wetland region. Forest and wetland net radiation measurements were implemented nearby in 1999 and 2000, respectively (Cook *et al.*, unpublished results). Comparison with data from the Willow Creek forest site shows that net radiation over the forest is typically about $100\,W\,m^{-2}$ greater than in the clearing (Baker *et al.*, this issue), so the net radiation data in Fig. 8 are likely to be systematically lower than the radiation driving the WLEF H and LE. We nevertheless expect a correlation between net radiation observed over the clearing and turbulent fluxes. To maximize the similarity between footprints, we limit the energy balance comparison to 30 m flux data which, during convective conditions, may be somewhat representative of the grassy clearing around the tower. Figure 8 shows excellent correlation between turbulent fluxes at 30 m and net radiation measured in the clearing. We have neglected storage and ground fluxes in this analysis. The ground heat flux is also difficult to estimate for the large WLEF footprint. Storage plus ground fluxes are typically of order 50–$100\,W\,m^{-2}$ at mid-day, roughly balancing our expected underestimate of net radiation. If these errors are offsetting, our degree of energy balance is roughly consistent with past eddy-covariance results over forests showing that $H + LE$ systematically underestimate net radiation by about 10–20% (Desjardins *et al.*, 1997).

Figure 9 shows the median diurnal pattern of LE observed at 122 m. The 122 m fluxes should show little to no influence of the clearing around the tower and the vertical flux divergence should be modest. Night-time LE is small at all levels, so using 30 m data does not add information at night. The general monthly pattern is very similar to the monthly course of CO_2 uptake shown in Fig. 6. One exception is that LE increases more rapidly in the spring compared to CO_2 uptake. This is likely caused by abundant solar radiation leading to evaporative fluxes in May prior to the early June onset of leaf-out, photosynthesis, and transpiration. A sum of the median monthly fluxes yields 367 mm as a rough estimate of total evapotranspiration for 1997, significantly less than the 668 mm of precipitation observed at Park Falls.

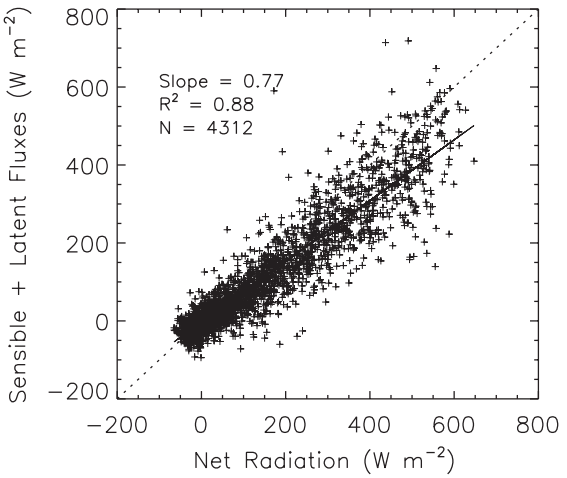

Fig. 8 Correlation between net radiation measured over the clearing immediately surrounding the WLEF tower and 30 m sensible plus latent heat turbulent fluxes. Each cross represents an hourly flux measurement. Data span days 97–365 of 1997. Net radiation measurements prior to day 97 showed anomalously small fluxes and were screened from this comparison. The dotted line is the 1 : 1 line, and the solid line is the orthogonal regression fit. Also shown are the slope of the fit, the coefficient of determination (R^2), and the number of points in the comparison (N). Note that the net radiation measurements are not representative of the forest around the tower and likely represent an underestimate of the fluxes driving the 30 m turbulent fluxes, see text.

Surface H increases to balance the surface energy budget when the vegetation is not transpiring. This, in combination with the lag between solar radiation and leaf cover, results in a strong seasonal pattern of Bowen ratio as shown in Fig. 10. Mid-day monthly median H peaks in April and May prior to leaf-out at about $200\,W\,m^{-2}$ and gradually decreases as transpiration and warming surface water tilt the surface energy balance in favor of LE as summer progresses. Periods of low Bowen ratio occur only when leaves are out, and correspond to the actual evapotranspiration approaching potential evapotranspiration, as defined by the

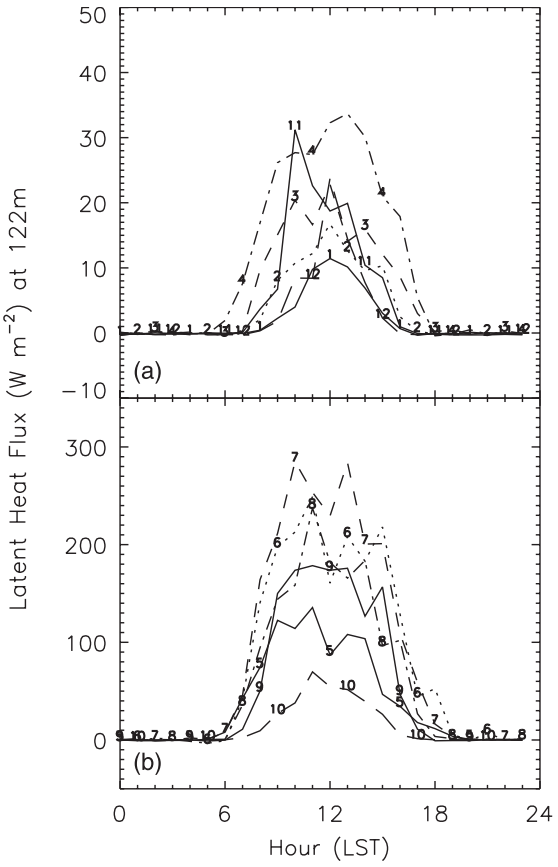

Fig. 9 Median monthly diurnal patterns of latent heat flux observed at 122 m at the WLEF tower in 1997. Only turbulent flux observations are shown. The months are divided into two plots, (a) dormant season and (b) growing season, to match Fig. 6. The curve for each month is labelled numerically where 1 = January, 2 = February, etc.

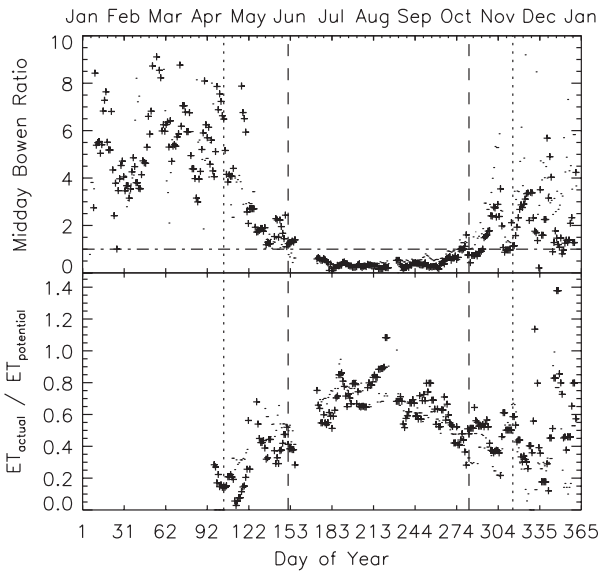

Fig. 10 Seven-day medians of mid-day (10–15 LST inclusive) (a) Bowen ratio, and (b) evapotranspiration normalized by potential evapotranspiration, as observed at the WLEF tower in 1997. Crosses show results derived from 122 m turbulent flux measurements. Dots, when distinguishable from the crosses, show results using 30 m turbulent flux data. Note that net radiation data prior to day 97 were screened out due to instrument errors, thus limiting the duration of the potential evapotranspiration estimate. Note also that the net radiation data are from the clearing around the tower, and that soil heat flux data are not available, thus the absolute value of the potential evapotranspiration estimate is subject to error. Vertical dashed lines indicate approximate dates of leaf-out and leaf-fall. Vertical dotted lines indicate soil thaw and freeze.

Priestly–Taylor equation (Stull, 1988). Thus despite abundant wetlands and surface water, the surface behaves as a water-limited environment in the absence of transpiring deciduous vegetation.

CO_2 mixing ratios and ABL budget

Finally, we compare the annual course of NEE of CO_2 and the ABL CO_2 mixing ratio. Figure 11 shows the cumulative integral of daily NEE of CO_2 as well as the annual pattern of CO_2 mixing ratio observed at the 396 m level. For much of the year, daily NEE of CO_2 (the slope of the cumulative NEE curve in Fig. 11) and the rate of change of CO_2 mixing ratio in the ABL are roughly consistent in their sign. That is, the net release of CO_2 corresponds to increasing ABL mixing ratios, and *vice versa*. There are two times of year, roughly May and September, when the signs of NEE of CO and $\partial CO_2/\partial t$ are very obviously contradictory. The seasonal evolution of the CO_2 mixing ratio precedes the tendency one would expect due to NEE of CO_2. This is strong evidence of large-scale vertical or horizontal advection of CO_2, presumably due to strong spatial gradients that have been created by the cumulative seasonal effect of net respiration from land in the winter and net uptake of CO_2 in the summer. Preliminary investigation of September of 1997 (Davis *et al.*, 2000) shows that the tendency for CO_2 to increase in fall counter to the influence of local NEE of CO_2 is due to discrete events where the mixing ratio increases rapidly at the time of a frontal passage. It is not yet clear whether this is due to vertical or horizontal transport. During fair weather, the ABL CO_2 mixing ratio trend seems to be governed by local NEE of CO_2.

Table 4 represents a simple effort to quantify this phase lag. The mean diurnal NEE of CO_2 at varying times is compared to the observed rate of change of the ABL CO_2 mixing ratio. The comparison is made by estimating the influence the observed, local NEE of CO_2

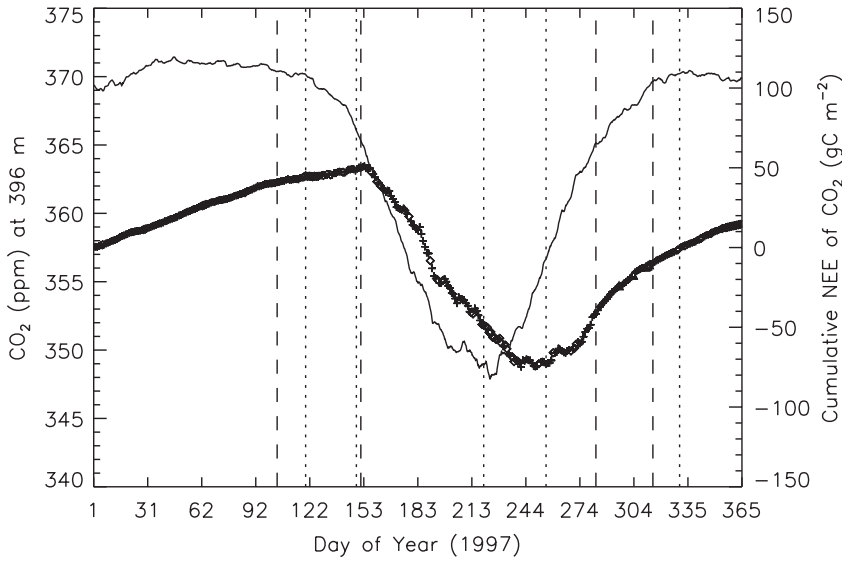

Fig. 11 CO_2 mixing ratio (solid line) and cumulative NEE of CO_2 (symbols) plotted as a function of day of the year. The mixing ratio curve is a 30-day running mean of daily mean CO_2 observations from 396 m. Each point on the cumulative NEE curve represents an increment of one day. Diamonds (crosses) indicate days where T_s–PAR fits were used to create more than (less than) 50% of the NEE data for that day. The dotted vertical lines denote the time intervals where mean values of $\partial CO_2/\partial t$ and NEE of CO_2 are compared in Table 4. The dashed vertical lines indicate the time of soil thaw, leaf-out, leaf-fall, and soil freeze, in that order, as determined from the data in Fig. 4.

Table 4 Observed rate of change of ABL CO_2 vs. that predicted by observed NEE of CO_2 and a simple budget Eqn (6); values are daily averages; the time intervals are illustrated in Fig. 11

			$\partial CO_2/\partial t$ estimated *via* NEE/z_{mix}		
Time interval (day of year)	NEE of CO_2 (g C m^{-2} day^{-1})	$\partial CO_2/\partial t$ observed (ppm $month^{-1}$)	$z_{mix} = 10$ km (ppm $month^{-1}$)	$z_{mix} = z_i$ (ppm day^{-1})	ABL depth (z_i) (km)
1–120 + 330–365	0.39	0.06	4.04	0.94	1.0
120–150	0.20	−4.68	2.07	0.24	2.0
150–220	−2.35	−6.96	−24.3	−2.83	2.0
220–255	−0.66	6.80	−6.83	−1.06	1.5
255–330	0.96	5.36	9.88	1.54	1.5

would have on the CO_2 mixing ratio of the boundary layer (depth about 1.5 km) or the entire troposphere (depth of 10 km) assuming a one-dimensional atmosphere. We say local NEE because the area of land that influences the time evolution of the atmospheric CO_2 mixing ratio is much larger than the flux footprint of the tower, even for the 396 m measurement level (Gloor *et al.*, 2001). This assumption of a one-dimensional atmosphere with no mixing from above leads to a simple expression for the expected time tendency of CO_2 as a function of NEE of CO_2. Given these assumptions, the scalar conservation equation becomes

$$\frac{\partial CO_2}{\partial t} = \frac{NEE_0^{CO_2}}{z,} \qquad (6)$$

where z is the characteristic mixing depth, which depends on the time scale. For periods of one to a few days the maximum boundary layer depth is a reasonable mixing depth since boundary layer air can remain fairly isolated from the troposphere for these periods. Synoptic weather and deep convection mix boundary layer air into the troposphere periodically so for time periods of weeks to months the depth of the troposphere is a more appropriate estimate of z. The NEE of CO_2 used in this calculation is the mean daily integral for the time of year since we are interested in the evolution of $\partial CO_2/\partial t$ over days not hours. The values of z_i used in Table 4 are approximate values based on measurements discussed by Yi *et al.* (2001).

The results of this simple calculation show that Eqn (6) is not satisfied at any time throughout the year, that is, vertical and/or horizontal transport of CO_2 are important terms in the budget of CO_2 in the ABL every month. The general trend that observed $\partial CO_2/\partial t$ leads the expected tendency due to NEE of CO_2 holds throughout the year. The imbalance between $\partial CO_2/\partial t$ and NEE reaches a maximum in summer when NEE is the largest and spatial gradients in CO_2 mixing ratio in the northern hemisphere probably also reach peak values. These data should provide a benchmark for models of atmospheric CO_2 fluxes and budgets that focus on continental and seasonal scales. Further investigation into the synoptic transport patterns that explain these data is warranted.

The predicted rates of change of CO_2 only for the boundary layer (Table 4) represent an estimate of how much we might expect the CO_2 content of an airmass moving across the continent to be modified each day. The values are substantial, and in fact underestimate observed synoptic trends (Davis *et al.*, 2000), probably because the NEE values represent monthly mean values. We conclude that observing the ABL CO_2 mixing ratio budget on a synoptic time scale is a readily accessible task. If merged with meteorological data assimilation methods, observations such as these may lead to regional to continental net CO_2 flux estimates for time periods as small as a few days (Baker *et al.*, this issue; Denning *et al.*, this issue).

Conclusions

Our best estimate of cumulative NEE of CO_2 observed at the WLEF tall tower site in northern Wisconsin in 1997 is 16 ± 19 g C $m^{-2} yr^{-1}$, hence the forest is nearly in carbon balance with the atmosphere. Estimates of GEP and total RE are large, 947 ± 18 and 963 ± 19 g C $m^{-2} yr^{-1}$, respectively. These error bars represent random uncertainty in the integrated fluxes. Systematic uncertainties in NEE that we could quantify are less than 60 g C $m^{-2} yr^{-1}$, fairly small compared to published values of NEE of CO_2 for temperate forest ecosystems. The systematic uncertainties in the GEP and RE values are 50–100 g C $m^{-2} yr^{-1}$. Included in this analysis was intercomparison among turbulent flux measurements made at 30, 122, and 396 m above ground. Identified systematic uncertainties include a bias towards small respiration fluxes at low u_* values (Goulden *et al.*, 1996a) and apparent persistent advective fluxes during the morning turbulence transition (Yi *et al.*, 2000). Imbalance of the surface energy budget is comparable to other forested sites.

The seasonal pattern of NEE of CO_2 is highly correlated with leaf-out and leaf-fall, and soil thaw and freeze. The seasonal pattern is similar to that of deciduous forest sites despite extensive wetlands and moderately abundant evergreen trees within the footprint of the WLEF tower. The rate of uptake of CO_2 during the growing season is smaller than has been reported for other deciduous forest sites (Aubinet *et al.*, 2000; Falge *et al.*, 2001). Wetlands or forest management may be responsible for the low rate of uptake.

NEE of water vapor largely follows the seasonal pattern of NEE of CO_2, with a lag in the spring when water vapor fluxes increase before CO_2 uptake, perhaps due to evaporation from standing water. The spring increase in sensible heat fluxes precedes the increase in evapotranspiration, resulting in large Bowen ratios in the spring. In general, the Bowen ratios are high during the dormant seasons and low during the growing season. Evapotranspiration normalized by potential evapotranspiration mirrors the Bowen ratio as evapotranspiration approaches its potential value during the growing season and drops during the dormant seasons.

The seasonal course of the ABL CO_2 mixing ratio at WLEF leads the seasonal pattern of NEE of CO_2 in time. This must be due to horizontal or vertical transport. Simple budget calculations show that at no time during the year is the seasonal evolution of CO_2 mixing ratio in balance with local NEE of CO_2. Transport and NEE of CO_2 are important components of the ABL CO_2 budget at all times of the year.

Acknowledgments

This research was funded in part by the National Institute for Global Environmental Change through the US Department of Energy, and by the Department of Energy's Terrestrial Carbon Processes program. Any opinions, findings, and conclusions or recommendations herein are those of the authors and do not necessarily reflect the views of DoE. This work would not have been possible without the gracious cooperation of the Wisconsin Educational Communications Board and Roger Strand (chief engineer for WLEF-TV). The carbon dioxide mixing ratio measurements, and site infrastructure and maintenance were supported by the Atmospheric Chemistry Project of the Climate and Global Change Program of the National Oceanic and Atmospheric Administration. This paper has benefited from the comments of two anonymous reviewers and D. Baldocchi.

References

Anthoni PM, Law BE, Unsworth MH (1999) Carbon and water vapor exchange of an open-canopied ponderosa pine ecosystem. *Agricultural and Forest Meteorology*, **95**, 151–168.

Aubinet M, Grelle A, Ibrom A *et al.* (2000) Estimates of the annual net carbon and water exchange of European forests: the EUROFLUX methodology. *Advances in Ecological Research*, **30**, 114–175.

Baker I, Denning AS, Hanan N *et al*. (this issue) Simulated and observed fluxes of sensible and latent heat and CO_2 at the WLEF-TV tower using SiB2.5. *Global Change Biology*, **9**, 1262–1267.

Bakwin PS, Tans PP, Hurst DF, Zhao C (1998) Measurements of carbon dioxide on very tall towers: results of the NOAA/CMDL program. *Tellus*, **50B**, 401–415.

Baldocchi D, Falge E, Gu L *et al*. (2001) FLUXNET: a new tool to study the temporal and spatial variability of ecosystem-scale carbon dioxide, water vapor and energy flux densities. *Bulletin of the American Meteorological Society*, **82**, 2415–2435.

Baldocchi DD, Hicks BB, Meyers TP (1988) Measuring biosphere–atmosphere exchanges of biologically related gases with micrometeorological methods. *Ecology*, **69**, 1331–1340.

Battle M, Ellis JT, Conway T *et al*. (2000) Global carbon sinks and their variability inferred from atmospheric O_2 and $\delta^{13}C$. *Science*, **287**, 2467–2470.

Berger BW, Davis KJ, Bakwin PS *et al*. (2001) Long-term carbon dioxide fluxes from a very tall tower in a northern forest: flux measurement methodology. *Journal of Atmospheric and Oceanic Technology*, **18**, 529–542.

Black TA, Chen WJ, Barr AG *et al*. (2000) Increased carbon sequestration by a boreal deciduous forest in years with a warm spring. *Geophysical Research Letters*, **27**, 1271–1274.

Bousquet P, Peylin P, Ciais P *et al*. (2000) Regional changes in carbon dioxide fluxes of land and oceans since 1980. *Science*, **290**, 1342–1346.

Caspersen JP, Moorcroft PR, Birdsey RA *et al*. (2000) Contributions of land-use history to carbon accumulation in U.S. forests. *Science*, **290**, 1148–1151.

Ciais P, Tans PP, Trolier M *et al*. (1995) A large Northern Hemisphere terrestrial CO_2 sink indicated by the $^{13}C/^{12}C$ ratio of atmospheric CO_2. *Science*, **269**, 1098–1102.

Conway TJ, Tans PP, Waterman LS *et al*. (1994) Evidence for interannual variability of the carbon cycle from the National Oceanic and Atmospheric Administration/Climate Monitoring and Diagnostics Laboratory Global Air Sampling Network. *Journal of Geophysical Research*, **99**, 22831–22855.

Cook BD, Davis KJ, Wang W, *et al*. (this issue) Annual pattern of carbon exchange and evapotranspiration from an upland deciduous forest in northern Wisconsin, in preparation.

Davis KJ, Yi C, Berger BW, *et al*. (2000) Scalar budgets in the continental boundary layer. Proceedings of the 14th Symposium on Boundary Layer and Turbulence, 7–11 August, American Meteorological Society, Aspen, CO, pp. 100–103.

Denning AS, Nicholls M, Prihodko L *et al*. (this issue) Simulated and observed variations in atmospheric CO_2 over a Wisconsin forest. *Global Change Biology*, in press.

Desjardins RL, MacPherson JI, Mahrt L *et al*. (1997) Scaling up flux measurements for the boreal forest using aircraft–tower combinations. *Journal of Geophysical Research*, **102**, 29125–29133.

Falge E, Baldocchi D, Olson RJ *et al*. (2001) Gap filling strategies for defensible annual sums of net ecosystem exchange. *Agricultural and Forest Meteorology*, **107**, 43–69.

Finnigan J (1999) A comment on the paper by Lee (1998): on micrometeorological observations of surface–air exchange over tall vegetation. *Agricultural and Forest Meteorology*, **97**, 55–64.

Francey RJ, Tans PP, Allison CE *et al*. (1995) Changes in oceanic and terrestrial carbon uptake since 1982. *Nature*, **373**, 326–330.

Gloor M, Bakwin P, Tans P *et al*. (2001) What is the concentration footprint of a tall tower? *Journal of Geophysical Research*, **106**, 17831–17840.

Goulden ML, Munger JW, Fan S-M *et al*. (1996a) Measurements of carbon sequestration by long-term eddy covariance: methods and a critical evaluation of accuracy. *Global Change Biology*, **2**, 169–182.

Goulden ML, Munger JW, Fan S-M *et al*. (1996b) Exchange of carbon dioxide by a deciduous forest: response to interannual climate variability. *Science*, **271**, 1576–1578.

Horst TW, Weil JC (1992) Footprint estimation for scalar flux measurements in the atmospheric surface layer. *Boundary-Layer Meteorology*, **59**, 279–296.

Houghton RA (1999) The annual net flux of carbon to the atmosphere from changes in land use 1850–1990. *Tellus*, **51B**, 298–313.

Keeling RF, Piper SC, Heimann M (1996) Global and hemispheric CO_2 sinks deduced from changes in atmospheric O_2 concentration. *Nature*, **381**, 218–221.

Lee X (1998) On micrometeorological observations of surface-air exchange over tall vegetation. *Agricultural and Forest Meteorology*, **91**, 39–49.

Lee X, Fuentes JD, Staebler RM *et al*. (1999) Long-term observation of the atmospheric exchange of CO_2 with a temperate deciduous forest in southern Ontario, Canada. *Journal of Geophysical Research*, **104**, 15975–15984.

Lenschow DH (1995) Micrometeorological techniques for measuring biosphere–atmosphere trace gas exchange. In: *Biogenic Trace Gases: Measuring Emissions from Soil and Water* (eds Pamela AM, Harriss RC), pp. 126–163. Chapter 5. Blackwell Science, Cambridge, MA.

Lindroth A, Grelle A, Moren A-S (1998) Long-term measurements of boreal forest carbon balance reveal large temperature sensitivity. *Global Change Biology*, **4**, 443–450.

Lloyd J, Taylor JA (1994) On the temperature dependence of soil respiration. *Functional Ecology*, **8**, 315–323.

Mackay DS, Ahl DE, Ewers BE *et al*. (2002) Aggregation effects of remotely sensed vegetation cover on estimates of evapotranspiration in a northern Wisconsin forest. *Global Change Biology*, **8**, 1253–1266.

Massman WJ, Lee X (2002) Eddy covariance flux corrections and uncertainties in long term studies of carbon and energy exchanges. *Agricultural and Forest Meteorology*, **113**, 121–144.

Pacala SW, Hurtt GC, Baker D *et al*. (2001) Consistent land- and atmosphere-based U.S. carbon sink estimates. *Science*, **292**, 2316–2319.

Pawu KT, Baldocchi DD, Meyers TP *et al*. (2000) Correction of eddy-covariance measurements incorporating both advective effects and density fluxes. *Boundary-Layer Meteorology*, **97**, 487–511.

Running SW, Gower ST, Bakwin PS *et al*. (1999) A global terrestrial monitoring network integrating tower fluxes, flask sampling, ecosystem modeling and EOS satellite data. *Remote Sensing of Environment*, **70**, 108–127.

Schlesinger WH (1997) *Biogeochemistry: An Analysis of Global Change*. Academic Press, San Diego, CA, USA.

Schmid HP, Grimmond CSB, Cropley F *et al*. (2000) Measurements of CO_2 and energy fluxes over a mixed hardwood forest in the mid-western United States. *Agricultural and Forest Meteorology*, **103**, 357–374.

Stull RB (1988) *An Introduction to Boundary Layer Meteorology*. Kluwer Academic Publishers, Dordrecht.

Tans PP, Fung IY, Takahashi T (1990) Observational constraints on the global atmospheric CO_2 budget. *Science*, **247**, 1431–1438.

Twine TE, Kustas WP, Norman JM *et al*. (1999) Correcting eddy-covariance flux underestimates over a grassland. *Agricultural and Forest Meteorology*, **103**, 279–300.

Valentini R, Rebmann C, Moors EJ *et al*. (2000) Respiration as the main determinant of carbon balance in European Forests. *Nature*, **404**, 861–865.

Weil JC, Horst TW (1992) Footprint estimates for atmospheric flux measurements in the convective boundary layer. In: *Precipitation Scavenging and Atmosphere–Surface Exchange*, **Vol. 2** (coords Schwartz SE, Slinn WGN), pp. 717–728. Hemisphere Publishing, Washington, DC.

Wilson KB, Baldocchi DD (2001) Comparing independent estimates of carbon dioxide exchange over 5 years at a deciduous forest in the southeastern United States. *Journal of Geophysical Research*, **106**, 34167–34178.

Wofsy SC, Goulden ML, Munger JW *et al*. (1993) Net exchange of CO_2 in a mid-latitude forest. *Science*, **260**, 1314–1317.

Yi C, Davis KJ, Bakwin PS *et al*. (2001) Long-term observations of the evolution of the planetary boundary layer. *Journal of the Atmospheric Sciences*, **58**, 1288–1299.

Yi C, Davis KJ, Bakwin PS *et al*. (2000) The influence of advection on measurements of the net ecosystem-atmosphere exchange of CO_2 observed from a very tall tower. *Journal of Geophysical Research*, **105**, 9991–9999.

Zhao CL, Bakwin PS, Tans PP (1997) A design for unattended monitoring of carbon dioxide on a very tall tower. *Journal of Atmospheric and Oceanic Technology*, **14**, 1139–1145.